Am J Transl Res 2024;16(4):1401-1414
www.ajtr.org /ISSN:1943-8141/AJTR0156252

Original Article

Circ_0072088 promotes breast carcinoma progression via modulating miR-607/RNF2 axis

Mingxi Chen[1], Yang Hui[2], Bo Tian[3]

[1]*Department of Surgery, Xi'an Hospital of Traditional Chinese Medicine, Xi'an 710021, Shaanxi, China;* [2]*Department of Surgical Oncology, Affiliated Hospital of Shaanxi University of Chinese Medicine, Xianyang 712000, Shaanxi, China;* [3]*Department of Surgery, Hospital of Northwestern Polytechnical University, Xi'an 710072, Shaanxi, China*

Received March 1, 2024; Accepted April 8, 2024; Epub April 15, 2024; Published April 30, 2024

Abstract: Objectives: To explore how the circular non-coding RNA circ_0072088 influences the progression of breast carcinoma (BC) by affecting cell behavior. Methods: We measured the levels of circ_0072088, microRNA-607 (miR-607), and ring finger protein 2 (RNF2) mRNA levels in BC tissues and cell lines using quantitative real-time PCR. We also conducted cell counting kit-8 (CCK-8), BrdU incorporation, and flow cytometry assays to assess cell viability, cell cycle, and apoptosis, respectively. Results: We observed increased levels of circ_0072088 and RNF2, and decreased levels of miR-607 in BC tissues. Overexpressing circ_0072088 promoted BC cell proliferation and cell cycle progression while inhibiting apoptosis. Conversely, silencing circ_0072088 had the opposite effects. Our data suggest that circ_0072088 directly targets and downregulates miR-607, which in turn upregulates RNF2, a target of miR-607. Moreover, miR-607 overexpression could mitigate the pro-proliferative and anti-apoptotic effects of circ_0072088 on BC cells. Conclusion: Circ_0072088 drives BC progression by downregulating miR-607 and upregulating RNF2, thereby promoting cell proliferation and cycle progression while reducing apoptosis.

Keywords: Breast carcinoma, circ_0072088, miR-607, ring finger protein 2

Introduction

Breast carcinoma (BC) is a major health threat for women, noted for its heterogeneity due to environmental and genetic factors [1, 2]. Despite the mainstay treatments of surgery and radiotherapy, challenges like distant metastases and chemotherapy resistance persist, leading to poor prognosis in some patients [3, 4]. This underscores the necessity to further understand BC pathogenesis and develop new diagnostic and therapeutic strategies.

Circular RNA (circRNA) molecules, which form a covalently closed loop structure, differ from traditional mRNA by lacking a 5' cap and a 3' Poly A tail. They are ubiquitous across eukaryotic cells and play roles in gene regulation, including miRNA sponging and translation modulation [5, 6]. The dysregulation of circRNAs has been linked to cancer development. For example, circ_0136666 is overexpressed in colorectal cancer, targeting miR-497 to promote PD-L1 expression, cell proliferation, and apoptosis inhibition [7]. In breast cancer, circ_0008673 upregulation has been tied to enhanced malignancy through miR-153-3p sponging, increasing CFL2 expression [8], with similar patterns observed in hepatic and non-small cell lung carcinomas [9, 10]. Our study focuses on hsa_circ_0072088 (circ_0072088), identified as upregulated in BC through circRNA microarray analysis (GSE101123), aiming to clarify its function and mechanisms in BC.

While miR-607 downregulation has been reported in various cancers, indicating its tumor-suppressive role, its relationship with BC and interaction with circRNAs like circ_0072088 remains unclear [11-13]. Additionally, the ring finger protein 2 (RNF2) has been associated with enhanced BC cell viability, colony formation, migration, and aggressiveness [14, 15], yet its potential regulation by circ_0072088 and miR-607 is not well documented. Our research investigates the expression and

Table 1. Primer sequences

	Primer Sequence (5'-3')
circ_0072088	Sense: TGATTTTCCAAGCTGGCCCT
	Antisense: TCTGAACTGCCTGTAACTCC
miR-607	Sense: GTTCAAATCCAGATCTATAAC
	Antisense: TGGTGTCGTGGAGTCG
RNF2	Sense: TCAGTGGGGTTAGGTACATTC
	Antisense: TTTACAAGTAGACAGCGGTGA
GAPDH	Sense: AAGGTCGGAGTCAACGGA
	Antisense: TTAAAAGCAGCCCTGGTGA
U6	Sense: CTCGCTTCGGCAGCACA
	Antisense: ACGCTTCACGAATTTGCGT

impact of circ_0072088 on BC cell growth, cycle progression, and apoptosis, proposing it as a potential as a therapeutic target for BC.

Materials and methods

Bioinformatics analysis

The microarray dataset (GSE101123) from the Gene Expression Omnibus (GEO) database (URL: https://www.ncbi.nlm.nih.gov/geo/) was analyzed to obtain BC (n=8) and noncancerous (n=3) samples [16, 17]. Differentially expressed circRNAs were identified using a threshold of $P < 0.05$ and an absolute log2 (fold change) > 1, visualized through heat maps and volcano plots. CircInteractome (https://circinteractome.nia.nih.gov/) was used to predict the binding site between circ_0072088 and miR-607. miRWalk (http://129.206.7.150/) and TargetScan (https://www.targetscan.org/vert_72/) helped identify miR-607 downstream targets of miR-607.

Tissue sample collection

Tissue samples from 48 BC patients, who had not undergone preoperative treatments, were collected at the Affiliated Hospital of Shaanxi University of Chinese Medicine between May 2019 and May 2021, with ethical approval. Post-surgery, tissues were immediately frozen in liquid nitrogen (-80°C).

Cell culture and transfection

BC cell lines (Hs 578T, HCC1937, ZR-75-1, MCF7, and MDA-MB-231) were obtained from the Cell Bank of Type Culture Collection Committee of the Chinese Academy of Sciences, Shanghai, China. The normal mammary epithelial cell line MCF-10A was acquired from the American Type Culture Collection (Rockville, MD, USA). BC cell lines were cultured in Dulbecco's Modified Eagle's Medium (DMEM) supplemented with 10% fetal bovine serum, 100 U/mL penicillin G, and 100 μg/mL streptomycin (all from Thermo Fisher Scientific, Waltham, MA, USA). MCF-10A cells were grown in Roswell Park Memorial Institute 1640 (RPMI1640) medium (Invitrogen, Carlsbad, CA, USA). All cells were maintained in a 37°C incubator with 5% CO_2 and 95% relative humidity.

Hs 578T and MCF7 were seeded in 6-well plates at 3 × 10^5 cells/well and cultured for 24 hours at 37°C. Upon reaching 70% confluence, cells were transfected with empty vector (negative control, NC), circ_0072088-overexpressing plasmid (circ_0072088-OE), siRNAs targeting circ_0072088 (si-circ_0072088#1 and si-circ_0072088#2), siRNA NC, miR-607 mimics, and inhibitors, along with their respective NCs, following Lipofectamine™ 2000 protocol (Invitrogen, Carlsbad, CA, USA). Transfection efficiency was evaluated 24 hours later using real-time quantitative polymerase chain reaction (RT-qPCR).

RT-qPCR

RNA from BC tissues and cells was extracted using Trizol Reagent and PARIS™ Kit, followed by cDNA synthesis using PrimeScript RT and miScript Reverse Transcription Kits. RT-qPCR was conducted on a CFX Connect Real-Time PCR Detection System using SYBR® Premix Ex TaqTM. Expression levels of circ_0072088, miR-607, and RNF2 mRNA were quantified against GAPDH and U6 using the 2-ΔΔCt method. Primer sequences are listed in **Table 1**.

RNase R digestion assay

Total RNA was extracted from Hs 578T and MCF7 cells and treated with 3 U/μg RNase R at 37°C for 15 minutes to digest linear RNAs. The stability of circ_0072088 was then evaluated using RT-qPCR.

Cell counting kit-8 (CCK-8) assay

For viability assessment, transfected MCF7 and Hs 578T cells were seeded in 96-well plates (2 × 10^4 cells/well) and incubated at

37°C for 24, 48, and 72 hours. At these time points, 10 μL of CCK-8 solution (Beyotime, Shanghai, C*hina*) was added to each well and incubated for 2 hours of cultivation at 37°C. Absorbance at 450 nm was measured using a microplate reader to determine cell viability.

5-bromo-2'-deoxyuridine (BrdU) assay

Proliferation was measured using a BrdU assay kit. Transfected MCF7 and Hs 578T cells were seeded in 96-well plates (5 × 10^3 cells/well) and incubated overnight. Cells were then labeled with 20 μL of BrdU solution for 12 hours of incubation at 37°C, fixed in 4% paraformaldehyde, and stained with anti-BrdU antibody. DAPI was used for nuclear staining. Fluorescence microscopy was used to capture images, and BrdU-positive cells were counted in three randomly selected fields.

Flow cytometry (FCM)

After transfection, MCF7 and Hs 578T cells were seeded into 6-well plates at a density of 5.0 × 10^5 cells per well and cultured for 24 hours. For cell cycle analysis, transfected cells were fixed in 75% ethanol overnight at 4°C, treated with an RNase A and 0.5% Triton X-100 for 30 minutes at 37°C in the dark, and stained with 400 μL of propidium iodide (PI). Cell cycle distribution was analyzed by FCM (BD Biosciences, San Jose, CA, USA).

An apoptosis assay was performed with an Annexin V-FITC/PI Apoptosis Kit (Invitrogen). Following trypsin digestion, cells were centrifuged by 5 minutes at 1500 r/min, and then resuspended in 500 μL of binding buffer. To this suspension, 10 μL of Annexin V-FITC and 5 μL of PI were added. The cells were then incubated for 15 minutes at room temperature in the dark. Following incubation, apoptosis levels were assessed using a flow cytometer (BD Biosciences).

Dual-luciferase reporter (DLR) gene assay

To analyze the interaction between miR-607 and circ_0072088 or RNF2, fragments containing miR-607 binding sites were cloned into pmirGLO vectors, generating wild-type (WT) and mutant-type (MUT) DLR vectors for circ_0072088 and RNF2. These constructs were subsequently co-transfected into MCF7 and Hs 578T cells along with miR-607 mimics or negative control (miR-NC) using Lipofectamine™ 2000. After 48 hours, luciferase activity was measured using a Dual-Luciferase Reporter Assay System (Promega, USA).

RNA immunoprecipitation (RIP) assay

We conducted an RNA immunoprecipitation (RIP) assay using Magna RIP RNA-binding protein immunoprecipitation kits (MilliporeSigma, Billerica, USA). MCF7 and Hs 578T cells (1 × 10^7) were collected and lysed using RIP lysis buffer containing protease and RNase inhibitors (MilliporeSigma). Then, 100 μL of the cell lysate was incubated overnight at 4°C with beads coated with either anti-IgG or anti-Ago2 antibodies (ab172730, ab186733, Abcam) as a negative control (NC). Following proteinase K treatment, the immunoprecipitated RNA was isolated using the RNeasy MinElute Cleanup Kit (QIAGEN GmbH, Germany). Finally, the levels of circ_0072088 and miR-607 were measured by RT-qPCR.

Western blot

To isolate total protein, BC cells were lysed with RIPA solution (Pierce Co. Manufacturers Ltd., IL, USA). The protein concentration was determined by a bicinchoninic acid kit (Pierce). For protein analysis, 30 μg of total protein was subjected to electrophoresis on an 8% sodium dodecyl sulfate-polyacrylamide gel, then transferred onto polyvinylidene fluoride membranes (Millipore) and blocked with 5% nonfat dry milk at room temperature for 2 hours. The membranes were incubated overnight at 4°C with anti-RNF2 and anti-GAPDH antibodies (diluted 1:500; ab101273, ab9485, Abcam). The next day, the membranes were incubated with a goat anti-rabbit IgG HRP-conjugated secondary antibody (ab205718, 1:3000, Abcam) for 1 hour, followed by band detection with an enhanced chemiluminescence (ECL) kit (Wuhan Servicebio Technology Co., Ltd., China) and band intensity quantification with Image J software (NIH Image, Bethesda, MD, USA).

Statistical analyses

SPSS 22.0 from SPSS (Inc., Chicago, IL, USA) was utilized for data analyses. Each assay was independently replicated three times, with the results described in the form of mean ± stan-

dard deviation (x ± SD). Pairwise comparisons were conducted with independent sample t-tests, while multiple group comparisons were made by one-way analysis of variance followed by Tukey's post-hoc test. Kaplan-Meier analysis was carried out to evaluate the association of circ_0072088 expression with BC patients' overall survival. Additionally, the correlation of circ_0072088 expression with BC patients' clinicopathological characteristics was determined by the chi-square test. Statistical significance was defined as *P*-values less than 0.05.

Results

Circ_0072088 expression is upregulated in BC cells

Analysis of the GEO microarray dataset GSE101123, we identified 149 differentially expressed circRNAs with differential expression in BC tissues, with 94 upregulated and 55 downregulated, using a cutoff of log2 |fold change| > 1 and P < 0.05 (**Figure 1A** and **1B**). circ_0072088 was significantly upregulated in BC tissues (**Figure 1C**) and BC cell lines (Hs 578T, HCC1937, ZR-75-1, MCF7, MDA-MB-231) compared to normal mammary epithelial MCF-10A cells (**Figure 1D**), as determined by RT-qPCR. The resistance of circ_0072088 to RNase R digestion confirmed its circular structure (**Figure 1E**). Subcellular localization studies showed circ_0072088 predominantly in the cytoplasm of BC cells (**Figure 1F**). Survival analysis linked higher circ_0072088 levels with reduced overall survival (**Figure 1G**), and elevated expression correlated with advanced tumor-node-metastasis (TNM) stage (**Table 2**).

Biological role of circ_0072088 in BC cells

The biological role of circ_0072088 in BC was investigated by transfecting Hs 578T cells with a circ_0072088 overexpression plasmid (circ_0072088-OE) and MCF7 cells with siRNAs targeting circ_0072088. RT-qPCR confirmed the transfection efficiency (**Figure 2A**). Si-circ_0072088#1, with higher knockdown efficiency, was used in further experiments. CCK-8 assays showed that overexpression of circ_0072088 increased viability in Hs 578T cells, while knockdown decreased viability in MCF7 cells (**Figure 2B**). BrdU assays indicated enhanced proliferation in Hs 578T cells with circ_0072088 overexpression and reduced proliferation in MCF7 cells with circ_0072088 knockdown (**Figure 2C** and **2D**). FCM analyses revealed that circ_0072088 overexpression in Hs 578T cells accelerated cell cycle progression and reduced apoptosis, whereas knockdown in MCF7 cells induced G0/G1 phase arrest and increased apoptosis (**Figure 2E-H**).

MiR-607 is a downstream target of circ_0072088

Analysis using the CircInteractome database suggested miR-607 as a potential target of circ_0072088 (**Figure 3A**). Data from The Cancer Genome Atlas (TCGA) showed downregulated miR-607 expression in breast invasive carcinoma (BRCA) tissue samples (**Figure 3B**). Dual-luciferase reporter assays indicated that miR-607 mimics reduced luciferase activity in cells transfected with WT circ_0072088 but not in those with MUT circ_0072088 (**Figure 3C**). RNA immunoprecipitation confirmed the association of both circ_0072088 and miR-607 with Ago2- in BC cells (**Figure 3D**). Moreover, circ_0072088 overexpression decreased miR-607 levels, while knockdown increased them (**Figure 3E**), and miR-607 was underexpressed in BC compared to adjacent normal tissues (**Figure 3F**), showing an inverse relationship with circ_0072088 expression (**Figure 3G**).

Circ_0072088 modulates BC cell viability and expedites cell-cycle progression through miR-607

Transfection experiments with miR-607 mimics in circ_0072088-overexpressing Hs 578T cells, and miR-607 inhibitors in MCF7 cells with circ_0072088 knockdown, demonstrated that the regulatory effects of the circ_0072088/miR-607 axis on BC cell proliferation, cycle progression, and apoptosis (**Figure 4A-H**). These findings suggest that circ_0072088 promotes BC cell growth and suppresses apoptosis by sponging miR-607.

Circ_0072088 regulates RNF2 expression via miR-607 sponging

miR-607 target analysis identified pathways and genes, including RNF2, associated with BC cell viability and metastasis (**Figure 5A** and **5B**). TCGA data indicated higher RNF2 expression in BRCA tissues (**Figure 5C**). TargetScan predic-

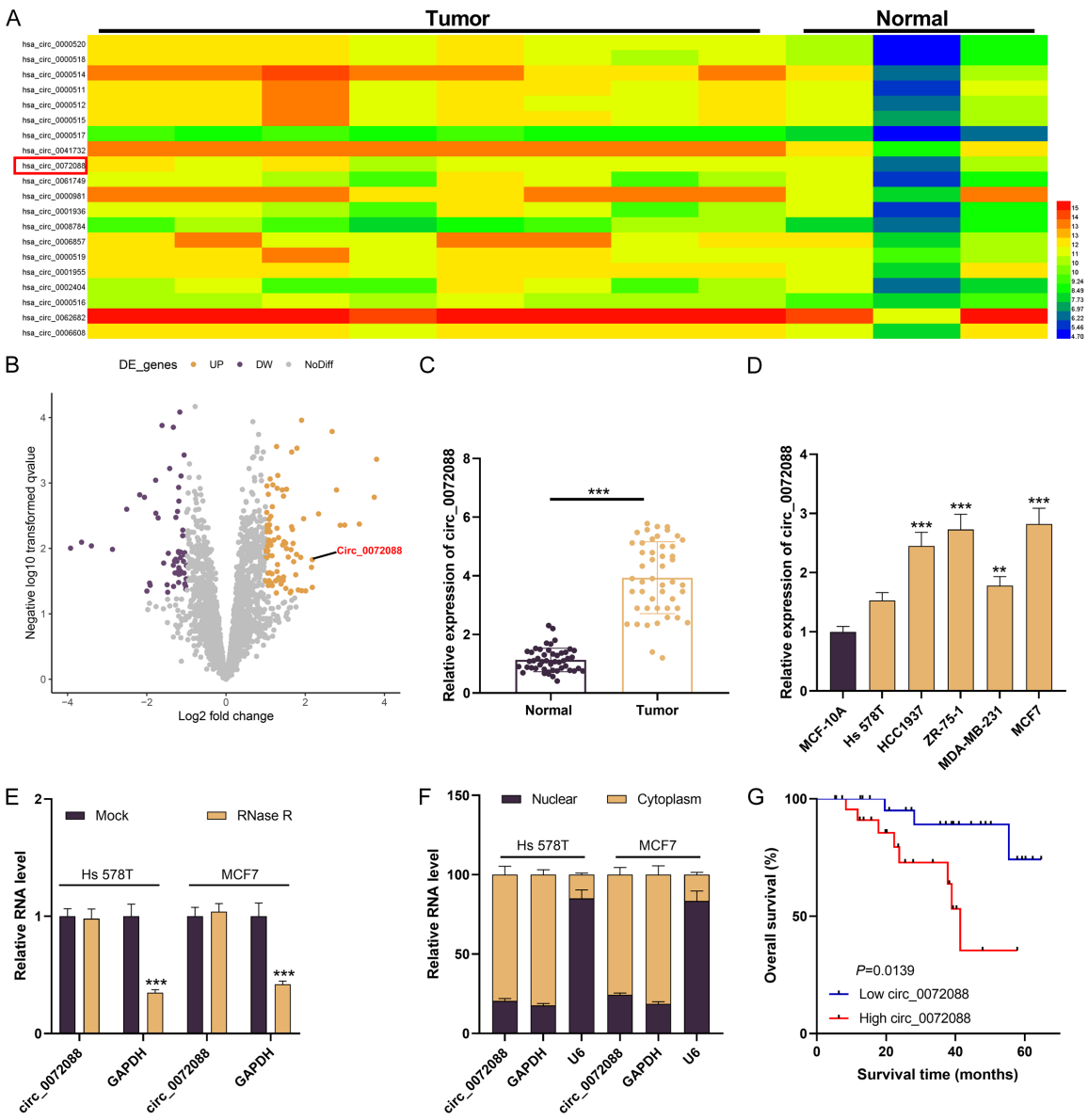

Figure 1. Circ_0072088 expression is increased in BC. A. The heat map revealed the expression profile of differentially expressed circRNAs in BC and normal tissues in dataset GSE101123. B. Volcano plots presented the differentially expressed circRNAs in the dataset GSE101123. The purple points represented down-regulated circRNAs, and the yellow points represented up-regulated ones. The gray points represented no statistically significant difference in circRNAs. C. circ_0072088 expressions in 48 BC tissues and normal counterparts were analyzed by RT-qPCR. D. Circ_0072088 expressions in normal breast epithelial MCF-10A cells and BC cell strains (Hs 578T, HCC1937, ZR-75-1, MCF7, and MDA-MB-231) were analyzed by RT-qPCR. E. The cyclical characteristics of circ_0072088 were detected by RNase R digestion assay. F. Subcellular fractionation assay was used to measure circ_0072088, U6, and GAPDH levels in the nuclear and cytoplasm of Hs 578T and MCF7. G. Kaplan-Meier curve was used to analyze the relationship between 0072088 and BC patients' overall survival. $^{**}P < 0.01$, and $^{***}P < 0.001$. BC, breast carcinoma.

tions and DLR assays confirmed miR-607's interaction with RNF2 3'UTR, affecting RNF2 expression (**Figure 5D** and **5E**). Western blot and RT-qPCR analyses showed that circ_0072088 overexpression upregulated RNF2, an effect reversed by transfection with miR-607 mimics. Conversely, circ_0072088 knockdown reduced RNF2 levels, which were restored by miR-607 inhibitors (**Figure 5F** and **5G**). Positive correlation between circ_0072088

Table 2. The correlation of circ_0072088 expression with clinicopathological features in breast cancer patients

Characteristics	Number (n=48)	circ_0072088 expression		χ^2	*P* value
		Low	High		
Age (years)					
≤ 50	21	10	11	0.085	0.771
> 50	27	14	13		
TNM stage					
I-II	19	13	6	4.267	0.039*
III-IV	29	11	18		
Tumor size					
≥ 5 cm	25	14	11	0.751	0.386
< 5 cm	23	10	13		
ER status					
Positive	22	12	10	0.336	0.562
Negative	26	12	14		
PR status					
Positive	20	9	11	0.343	0.558
Negative	28	15	13		
HER-2 status					
Positive	19	11	8	0.784	0.376
Negative	29	13	16		
Molecular subtype					
Luminal like	20	9	11	0.625	0.732
HER-2 positive	11	6	5		
Triple negative	17	9	8		

Note: TNM, Tumor-Node-Metastasis; ER, Estrogen Receptor; HER-2, Human Epidermal growth factor Receptor 2; *$P < 0.05$.

and RNF2 mRNA, and an inverse relationship between miR-607 and RNF2 mRNA in BC tissues, were observed (**Figure 5H** and **5I**).

Discussion

CircRNAs are stable, conserved non-coding RNAs with tissue-specific expression and resistance to RNA exonuclease degradation [18-21]. They are implicated in various human diseases, including cancer, and influence cell functions like growth, migration, autophagy, and apoptosis [22, 23]. Specifically, circRNAs play a significant role in BC progression [24]. For example, circ_000911 expression is reduced in BC tissues, and its overexpression has been observed to decrease cell viability, migration, and invasiveness while promoting apoptosis [25]. In contrast, CircGFRA1 levels are increased in triple-negative breast cancer (TNBC), correlating with larger tumor size, advanced TNM stage, lymph node metastasis, and higher histological grade [26]. Similarly, in hepatocellular carcinoma, elevated circ_0072088 expression has been linked to enhanced malignancy and reduced apoptosis [27]. In our research, we found that circ_0072088 is overexpressed in BC cells using the GSE101123 dataset analysis. Overexpression of circ_0072088 led to faster BC cell growth and cell cycle progression while inhibiting apoptosis, whereas silencing circ_0072088 showed opposite effects, indicating circ_0072088's role in promoting BC progression.

MicroRNAs (miRNAs) are conserved, endogenous, non-coding single-stranded RNA molecules that regulate gene expression post-transcriptionally through base pairing with the 3'UTR of target genes, leading to mRNA degradation or translational repression. These molecules are crucial for various biological processes, including cardiac and neurological development, and play a significant role in tumor progression [28-30]. Notably, miRNAs are not only pivotal in regulating processes such as cardiac

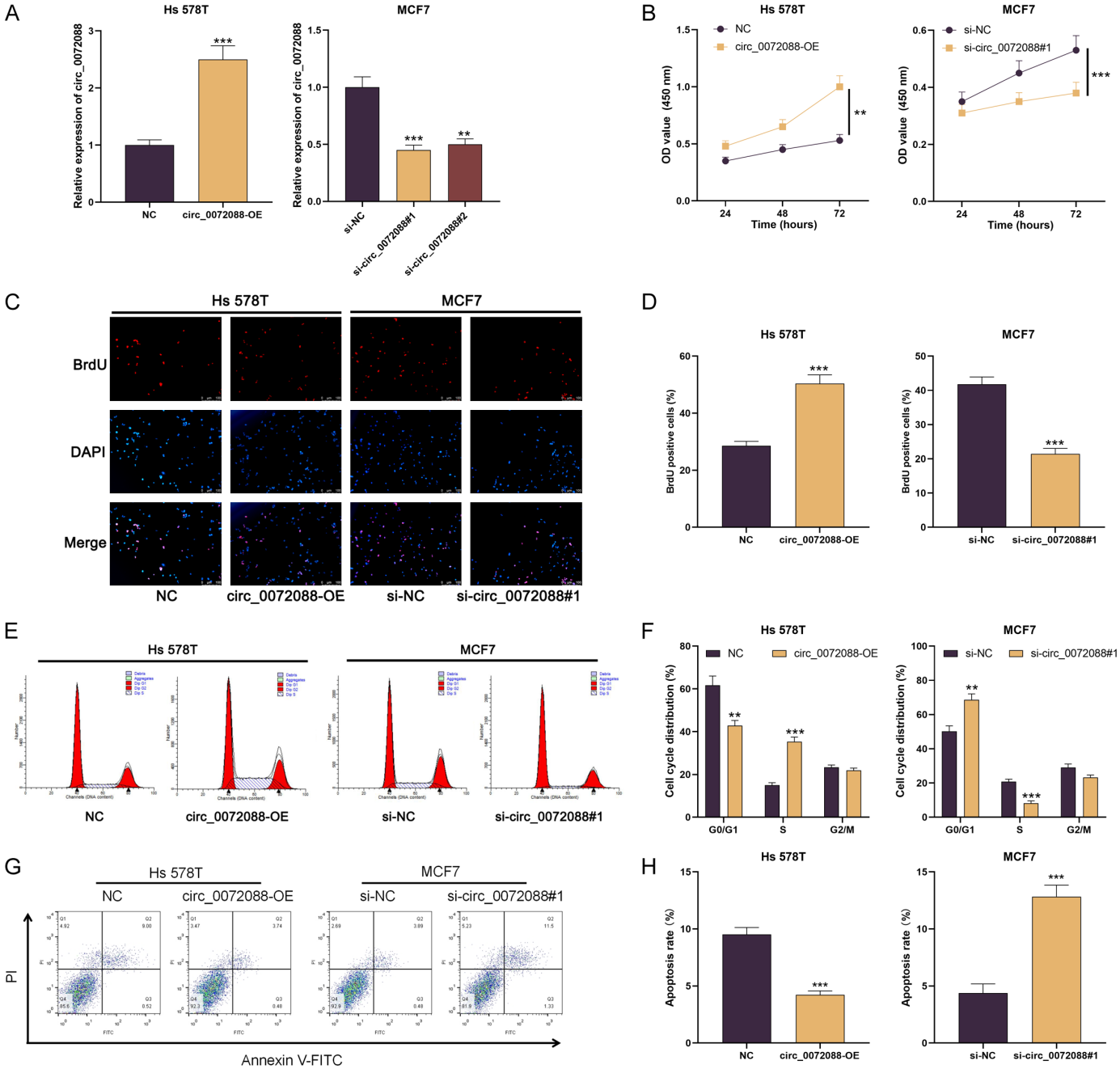
A
Hs 578T
MCF7
Relative expression of circ_0072088
NC
circ_0072088-OE
si-NC
si-circ_0072088#1
si-circ_0072088#2
B
Hs 578T
MCF7
NC
circ_0072088-OE
si-NC
si-circ_0072088#1
OD value (450 nm)
Time (hours)
C
Hs 578T
MCF7
BrdU
DAPI
Merge
NC
circ_0072088-OE
si-NC
si-circ_0072088#1
D
Hs 578T
MCF7
BrdU positive cells (%)
E
Hs 578T
MCF7
F
Cell cycle distribution (%)
G0/G1
S
G2/M
G
PI
Annexin V-FITC
H
Apoptosis rate (%)

Figure 2. Biological function of circ_0072088 in BC cells. The circ_0072088 overexpression plasmid was transfected into Hs 578T cells and si-circ_0072088#1 and #2 into MCF7 cells for 48 h of culture. A. The transfection efficiency of Hs 578T and MCF7 was tested using RT-qPCR. B-D. CCK-8 and BrdU assays determined the effects of circ_0072088 overexpression or knockdown on Hs 578T and MCF7 cell viability. E-H. Flow cytometry analyzed the effects of circ_0072088 overexpression or knockdown on Hs 578T and MCF7 cell cycles and apoptosis. $**P < 0.01$, and $***P < 0.001$. BC, breast carcinoma.

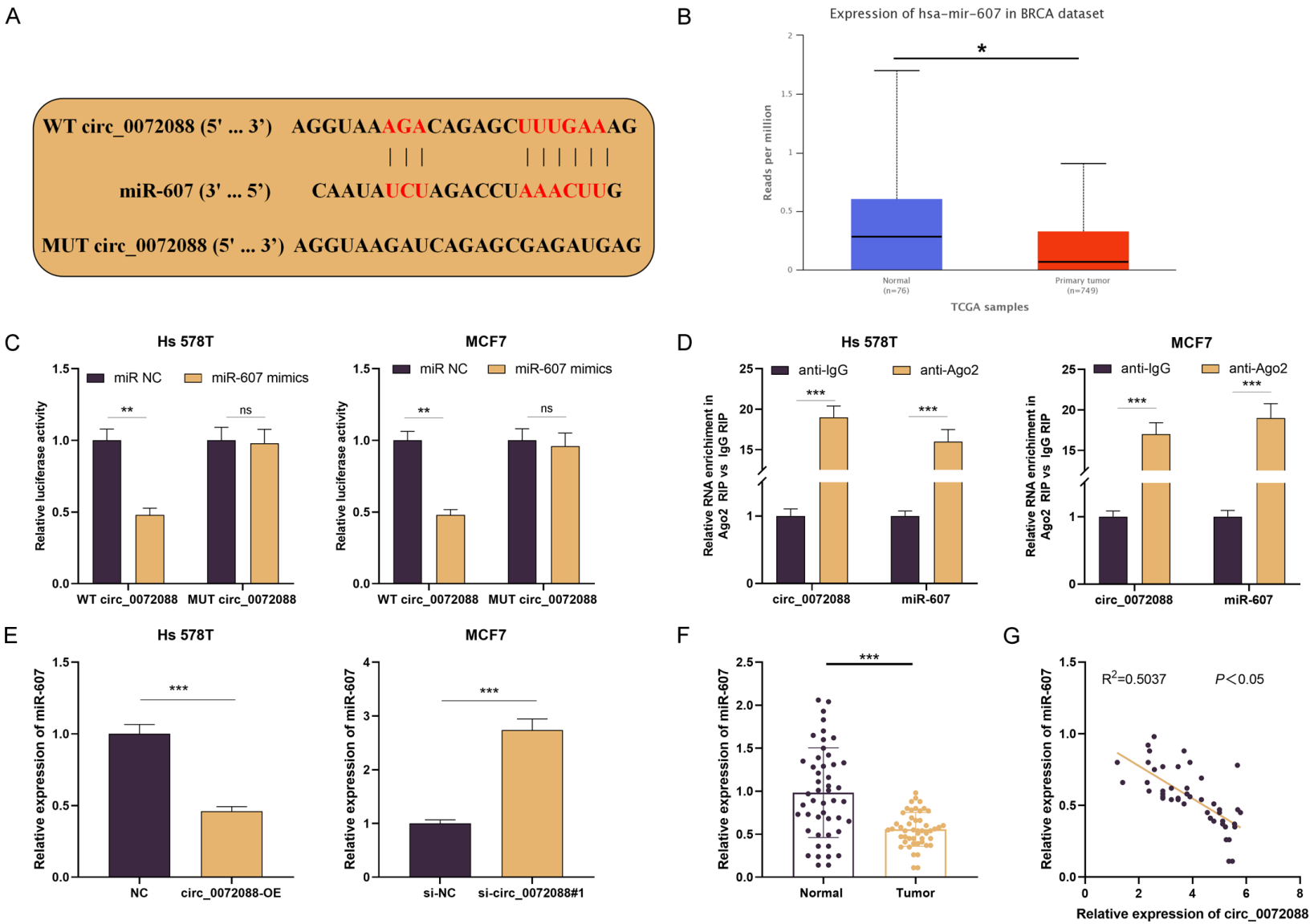

Figure 3. MiR-607 is a downstream target of circ_0072088. A. Binding site prediction between circ_0072088 and miR-607 was performed by the CircInteractome online database. B. MiR-607 expression in BRCA was analyzed by the TCGA database. C. After co-transfection of circ_0072088 WT and MUT with miR-607 mimics or the negative control (miR-NC) into Hs 578T and MCF7, respectively, a dual-luciferase reporter gene assay was performed to measure the relative luciferase activity. D. RIP assay analyzed the interplay between circ_0072088 and miR-607 in BC cells. E. RT-qPCR was employed to clarify the effect of circ_0072088 overexpression or knockdown on miR-607 expression. F. RT-qPCR exposed miR-607 expression in 48 BC and adjacent tissue samples. G. The interrelation between miR-607 and circ_0072088 expression in BC tissues was identified by Pearson's correlation analysis. *P < 0.05, **P < 0.01, and ***P < 0.001; ns, no statistical significance. BC, breast carcinoma; BRCA, breast invasive carcinoma; WT, wild type; MUT, mutant type.

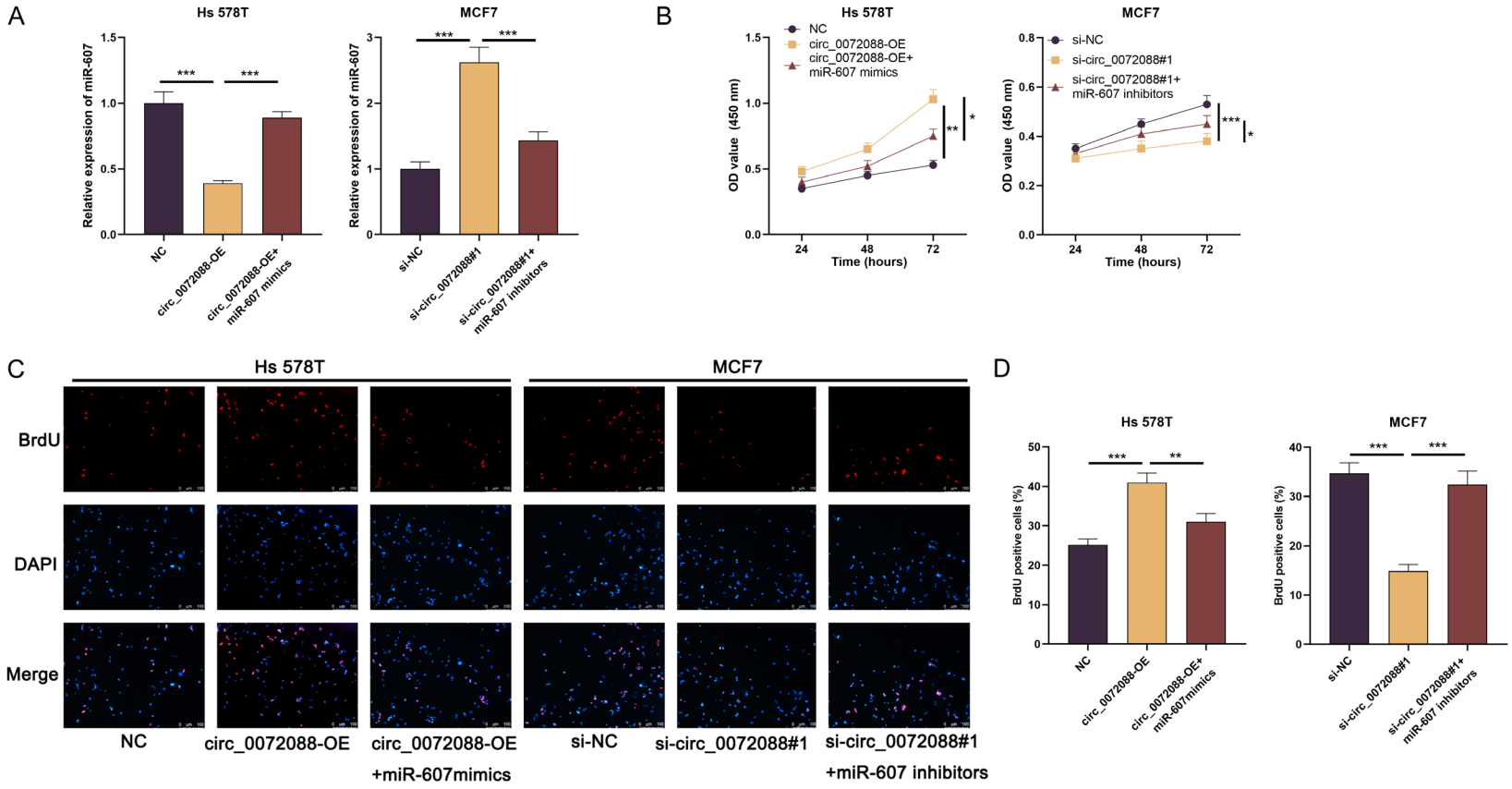

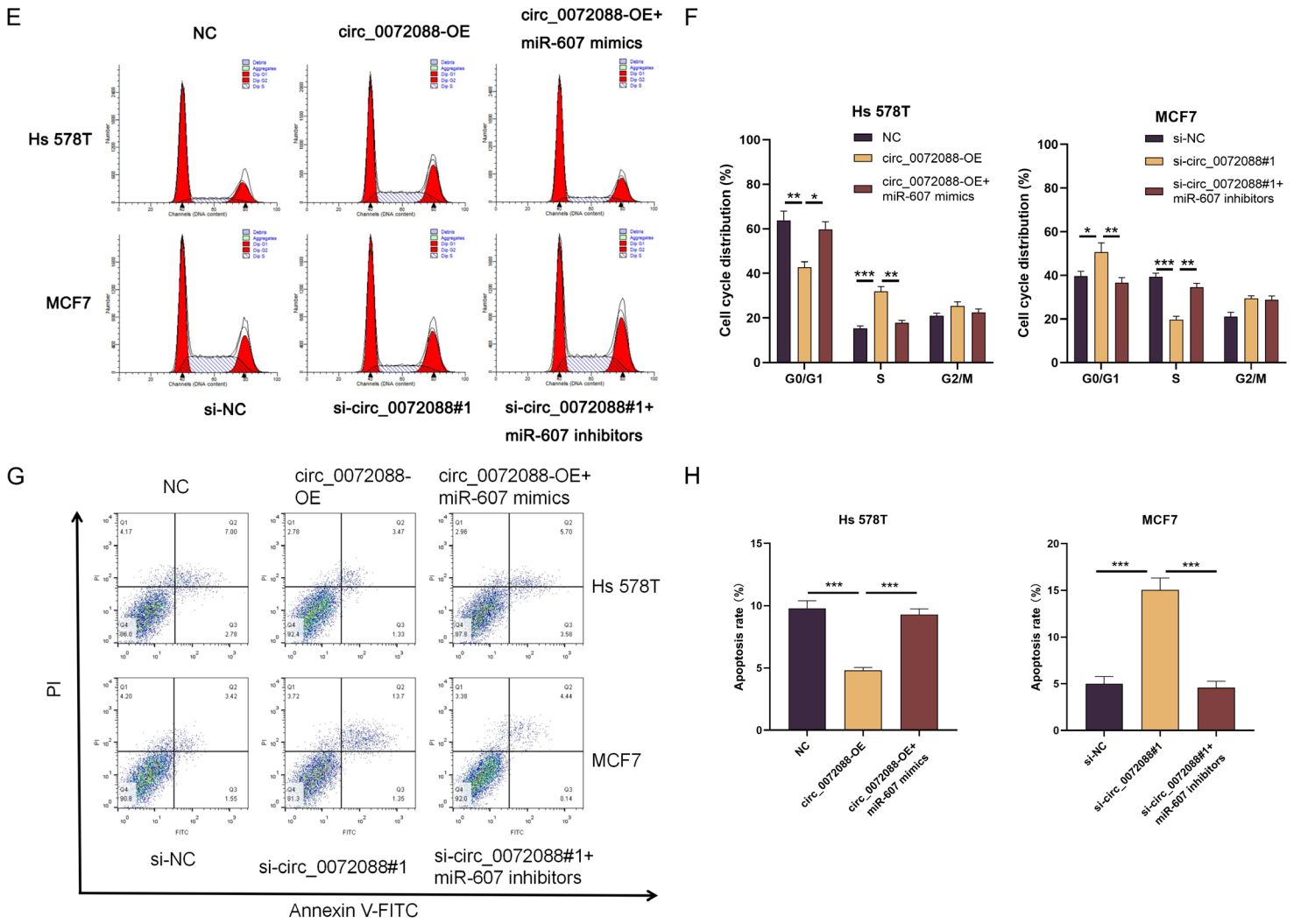

Figure 4. Impacts of circ_0072088 and miR-607 on BC cell biological functions. NC, circ_0072088-OE, and circ_0072088-OE+miR-607 mimics were transfected into Hs 578T cells, respectively; si-NC, si-circ_0072088#1, and si-circ_0072088#1+miR-607 inhibitors were transfected into MCF7 cells, respectively. (A) MiR-607 expressions in transfected Hs 578T and MCF7 cells were determined by RT-qPCR. (B-D) Hs 578T and MCF7 cell multiplication was evaluated with CCK-8 (B) and BrdU assays (C, D). (E-H) Flow cytometry was utilized to analyze Hs 578T and MCF7 cell-cycle distribution (E, F) and apoptosis (G, H). *P < 0.05, **P < 0.01, and ***P < 0.001. BC, breast carcinoma; BRCA, breast invasive carcinoma.

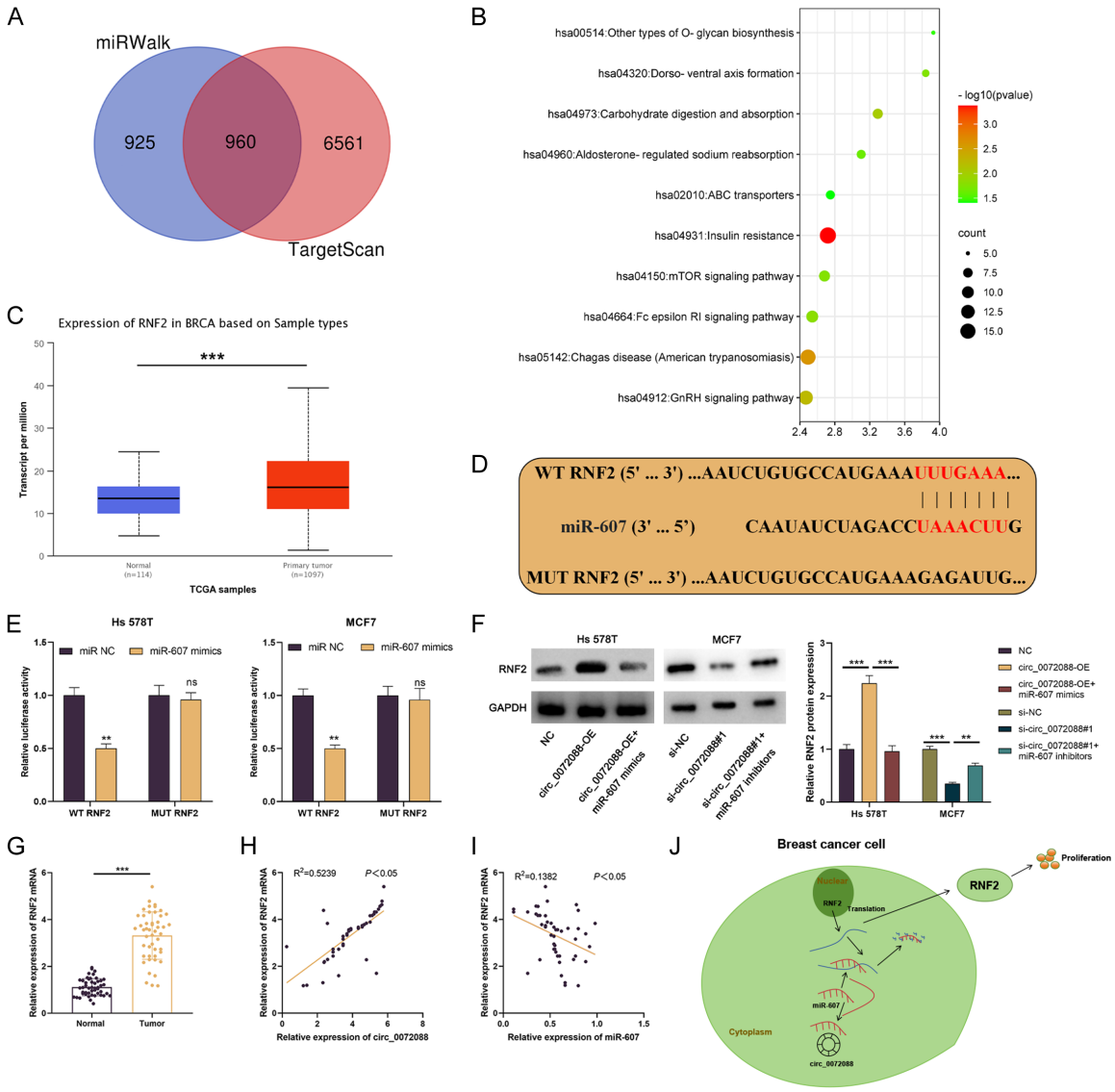

Figure 5. Circ_0072088 upregulates RNF2 by sponging miR-607. A and B. miRWalk, TargetScan, and David were utilized to identify target genes downstream of miR-607. C. RNF2 levels in BRCA and normal tissue samples were analyzed by the TCGA online database. D. The TargetScan online database predicted the binding loci between miR-607 and RNF2 mRNA 3'UTR. E. After co-transfection of WT RNF2 and MUT RNF2 with miR-607 mimics and the negative control (miR-NC) into Hs 578T and MCF7, luciferase activity determination was conducted with a dual-luciferase reporter assay. F. Western blotting was carried out to detect the impact of circ_0072088 and miR-607 on RNF2 expressions. G. RNF2 mRNA expression in BC and adjacent tissue samples were detected with RT-qPCR. H and I. The interplay between circ_0072088 and RNF2 mRNA, or miR-607 and RNF2 mRNA expression in BC tissues was subjected to Pearson's correlation analysis. J. A schematic model of circ_0072088/miR-607/RNF2 axis in BC. $^{**}P < 0.01$, and $^{***}P < 0.001$; ns, no statistical significance. BC, breast carcinoma; BRCA, breast invasive carcinoma; WT, wild type; MUT, mutant-type; RNF2, ring finger protein 2.

and neurological development but also intimately associated with tumor progression [31, 32]. For instance, miR-155-5p, upregulated in lung squamous carcinoma cells, enhances cell viability and invasiveness by downregulating fibroblast growth factor 9 [33]. Conversely, reduced miR-133b levels in TNBC inhibit cell growth by targeting FGFR1 and blocking the Wnt-β-catenin pathway [34]. Additionally, circRNAs, acting as miRNA sponges, modulate cancer progression [35]. In BC, circ_0084927 promotes cell growth and migration while inhibiting apoptosis by sponging miR-142-3p [36], and circ_0000284 advances malignancy by sponging miR-326 [37]. Our research reveals that circ_0072088 acts as a miR-607 sponge,

inversely affecting miR-607 levels in BC cells and promoting oncogenic activities like enhanced cell growth and altered cell cycle progression. Thus, circ_0072088, targeted by miR-607, plays a significant role in facilitating BC progression.

RNF2, a ubiquitin ligase with a finger-loop structure, is part of the protein family of proteins that ubiquitinates lysine at position 119 of histone H2A, influencing chromatin structure and gene repression [38]. Its elevated expression has been linked to the progression of various tumors, including gastric carcinoma, melanoma, and pancreatic carcinomas, and is associated with poor prognosis in skin squamous cell carcinoma [38, 39]. In BC, increased RNF2 levels have been observed and implicated in altering cellular processes [40]. RNF2 is also regulated by miRNAs, such as miR-539-3p and miR-149-5p [41, 42]. This study identifies RNF2 as a direct target of miR-607, with circ_0072088 acting as a miR-607 sponge, thus positively influencing RNF2 expression via a competitive endogenous RNA mechanism, and suggesting a role in BC progression (**Figure 5J**).

However, our study has limitations, including the need to clarify the specific relationship between the cell cycle and apoptosis in BC, investigate other biological behaviors like invasion and migration, and validate the impact of circ_0072088 on patient survival with larger cohorts. Further research is essential to elucidate circ_0072088's role in BC.

Conclusion

Our study confirms circ_0072088's upregulation in both BC tissues and cells and elucidates its mechanism of action. circ_0072088 enhances RNF2 expression by sponging miR-607, facilitating BC cell proliferation, cell-cycle progression, and apoptosis inhibition. These results underscore circ_0072088's potential as a diagnostic marker and therapeutic target in BC.

Disclosure of conflict of interest

None.

Address correspondence to: Bo Tian, Department of Surgery, Hospital of Northwestern Polytechnical University, Xi'an 710072, Shaanxi, China. Tel: +86-13892901281; E-mail: tianbodr@foxmail.com

References

[1] Li M, Zou X, Xia T, Wang T, Liu P, Zhou X, Wang S and Zhu W. A five-miRNA panel in plasma was identified for breast cancer diagnosis. Cancer Med 2019; 8: 7006-7017.

[2] Sung H, Ferlay J, Siegel RL, Laversanne M, Soerjomataram I, Jemal A and Bray F. Global cancer statistics 2020: GLOBOCAN estimates of incidence and mortality worldwide for 36 cancers in 185 countries. CA Cancer J Clin 2021; 71: 209-249.

[3] Mampre D, Mehkri Y, Rajkumar S, Sriram S, Hernandez J, Lucke-Wold B and Chandra V. Treatment of breast cancer brain metastases: radiotherapy and emerging preclinical approaches. Diagnostics and Therapeutics 2022; 1: 25.

[4] Yang W, Gong P, Yang Y, Yang C, Yang B and Ren L. Circ-ABCB10 contributes to paclitaxel resistance in breast cancer through Let-7a-5p/DUSP7 axis. Cancer Manag Res 2020; 12: 2327-2337.

[5] Huang JL, Xu ZH, Yang SM, Yu C, Zhang F, Qin MC, Zhou Y, Zhong ZG and Wu DP. Identification of differentially expressed profiles of Alzheimer's disease associated circular RNAs in a Panax notoginseng saponins-treated Alzheimer's disease mouse model. Comput Struct Biotechnol J 2018; 16: 523-531.

[6] Zhang L and Wang Z. Circular RNA hsa_circ_0004812 impairs IFN-induced immune response by sponging miR-1287-5p to regulate FSTL1 in chronic hepatitis B. Virol J 2020; 17: 40.

[7] Xu YJ, Zhao JM, Gao C, Ni XF, Wang W, Hu WW and Wu CP. Hsa_circ_0136666 activates Treg-mediated immune escape of colorectal cancer via miR-497/PD-L1 pathway. Cell Signal 2021; 86: 110095.

[8] Zhang L, Zhang W, Zuo Z, Tang J, Song Y, Cao F, Yu X, Liu S and Cai X. Circ_0008673 regulates breast cancer malignancy by miR-153-3p/CFL2 axis. Arch Gynecol Obstet 2022; 305: 223-232.

[9] Lin Y, Zheng ZH, Wang JX, Zhao Z and Peng TY. Tumor cell-derived exosomal circ-0072088 suppresses migration and invasion of hepatic carcinoma cells through regulating MMP-16. Front Cell Dev Biol 2021; 9: 726323.

[10] Zhang L, Wu Y, Hou C and Li F. Circ_0072088 knockdown contributes to cisplatin sensitivity and inhibits tumor progression by miR-944/LASP1 axis in non-small cell lung cancer. J Gene Med 2022; 24: e3414.

[11] Mo WL, Deng LJ, Cheng Y, Yu WJ, Yang YH and Gu WD. Circular RNA hsa_circ_0072309 promotes tumorigenesis and invasion by regulating the miR-607/FTO axis in non-small cell

lung carcinoma. Aging (Albany NY) 2021; 13: 11629-11645.
[12] Qiao G, Wang HB, Duan XN and Yan XF. The effect and mechanism of miR-607/CANT1 axis in lung squamous carcinoma. Anticancer Drugs 2021; 32: 693-702.
[13] Zhang H, Xue B, Wang S, Li X and Fan T. Long non-coding RNA TP73 antisense RNA 1 facilitates the proliferation and migration of cervical cancer cells via regulating microRNA-607/cyclin D2. Mol Med Rep 2019; 20: 3371-3378.
[14] Al-Raawi D, Jones R, Wijesinghe S, Halsall J, Petric M, Roberts S, Hotchin NA and Kanhere A. A novel form of JARID2 is required for differentiation in lineage-committed cells. EMBO J 2019; 38: e98449.
[15] Wu J, Wang H, Li Q, Guo QY, Tao SQ, Shen YX and Wu ZS. The oncogenic impact of RNF2 on cell proliferation, invasion and migration through EMT on mammary carcinoma. Pathol Res Pract 2019; 215: 152523.
[16] Xu JZ, Shao CC, Wang XJ, Zhao X, Chen JQ, Ouyang YX, Feng J, Zhang F, Huang WH, Ying Q, Chen CF, Wei XL, Dong HY, Zhang GJ and Chen M. circTADA2As suppress breast cancer progression and metastasis via targeting miR-203a-3p/SOCS3 axis. Cell Death Dis 2019; 10: 175.
[17] Zhou Y, Liu X, Lan J, Wan Y and Zhu X. Circular RNA circRPPH1 promotes triple-negative breast cancer progression via the miR-556-5p/YAP1 axis. Am J Transl Res 2020; 12: 6220-6234.
[18] Guo JU, Agarwal V, Guo H and Bartel DP. Expanded identification and characterization of mammalian circular RNAs. Genome Biol 2014; 15: 409.
[19] Jeck WR, Sorrentino JA, Wang K, Slevin MK, Burd CE, Liu J, Marzluff WF and Sharpless NE. Circular RNAs are abundant, conserved, and associated with ALU repeats. RNA 2013; 19: 141-157.
[20] Salzman J, Gawad C, Wang PL, Lacayo N and Brown PO. Circular RNAs are the predominant transcript isoform from hundreds of human genes in diverse cell types. PLoS One 2012; 7: e30733.
[21] Wilusz JE and Sharp PA. Molecular biology. A circuitous route to noncoding RNA. Science 2013; 340: 440-441.
[22] Lei K, Bai H, Wei Z, Xie C, Wang J, Li J and Chen Q. The mechanism and function of circular RNAs in human diseases. Exp Cell Res 2018; 368: 147-158.
[23] Zhu LP, He YJ, Hou JC, Chen X, Zhou SY, Yang SJ, Li J, Zhang HD, Hu JH, Zhong SL, Zhao JH and Tang JH. The role of circRNAs in cancers. Biosci Rep 2017; 37: BSR20170750.
[24] Chu M, Fang Y and Jin Y. CircRNAs as promising biomarker in diagnosis of breast cancer: an updated meta-analysis. J Clin Lab Anal 2021; 35: e23934.
[25] Wang H, Xiao Y, Wu L and Ma D. Comprehensive circular RNA profiling reveals the regulatory role of the circRNA-000911/miR-449a pathway in breast carcinogenesis. Int J Oncol 2018; 52: 743-754.
[26] He R, Liu P, Xie X, Zhou Y, Liao Q, Xiong W, Li X, Li G, Zeng Z and Tang H. circGFRA1 and GFRA1 act as ceRNAs in triple negative breast cancer by regulating miR-34a. J Exp Clin Cancer Res 2017; 36: 145.
[27] Li L, Xiao C, He K and Xiang G. Circ_0072088 promotes progression of hepatocellular carcinoma by activating JAK2/STAT3 signaling pathway via miR-375. IUBMB Life 2021; 73: 1153-1165.
[28] Chen LL. The biogenesis and emerging roles of circular RNAs. Nat Rev Mol Cell Biol 2016; 17: 205-211.
[29] Fang G, Jia X, Li H, Tan S, Nie Q, Yu H and Yang Y. Characterization of microRNA and mRNA expression profiles in skin tissue between early-feathering and late-feathering chickens. BMC Genomics 2018; 19: 399.
[30] Thomas LF and Sætrom P. Circular RNAs are depleted of polymorphisms at microRNA binding sites. Bioinformatics 2014; 30: 2243-2246.
[31] Katayama K, Nakashima S, Ishida H, Kubota Y, Nakano M, Fukami T, Sasaki Y, Fujita KI and Nakajima M. Characteristics of miRNA-SNPs in healthy Japanese subjects and non-small cell lung cancer, colorectal cancer, and soft tissue sarcoma patients. Noncoding RNA Res 2021; 6: 123-129.
[32] Mundalil Vasu M, Anitha A, Thanseem I, Suzuki K, Yamada K, Takahashi T, Wakuda T, Iwata K, Tsujii M, Sugiyama T and Mori N. Serum microRNA profiles in children with autism. Mol Autism 2014; 5: 40.
[33] Liu F, Mao Q, Zhu S and Qiu J. MicroRNA-155-5p promotes cell proliferation and invasion in lung squamous cell carcinoma through negative regulation of fibroblast growth factor 9 expression. J Thorac Dis 2021; 13: 3669-3679.
[34] Lin Y, Lin F, Anuchapreeda S, Chaiwongsa R, Duangmano S, Ran B and Pornprasert S. Effect of miR-133b on progression and cisplatin resistance of triple-negative breast cancer through FGFR1-Wnt-β-catenin axis. Am J Transl Res 2021; 13: 5969-5984.
[35] Gu Y, Wu F, Wang H, Chang J, Wang Y and Li X. Circular RNA circARPP21 acts as a sponge of miR-543 to suppress hepatocellular carcinoma by regulating LIFR. Onco Targets Ther 2021; 14: 879-890.

[36] Gong G, She J, Fu D, Zhen D and Zhang B. Circular RNA circ_0084927 regulates proliferation, apoptosis, and invasion of breast cancer cells via miR-142-3p/ERC1 pathway. Am J Transl Res 2021; 13: 4120-4136.
[37] Qi L, Sun B, Yang B and Lu S. circHIPK3 (hsa_circ_0000284) promotes proliferation, migration and invasion of breast cancer cells via miR-326. Onco Targets Ther 2021; 14: 3671-3685.
[38] Ling B, Yao M, Li G, Liu J, Liu B, Wang W and Jiang B. Clinical significance of ring finger protein 2 high expression in skin squamous cell carcinoma. Oncol Lett 2020; 20: 1111-1118.
[39] Yan Q, Chen BJ, Hu S, Qi SL, Li LY, Yang JF, Zhou H, Yang CC, Chen LJ and Du J. Emerging role of RNF2 in cancer: from bench to bedside. J Cell Physiol 2021; 236: 5453-5465.
[40] Bosch A, Panoutsopoulou K, Corominas JM, Gimeno R, Moreno-Bueno G, Martín-Caballero J, Morales S, Lobato T, Martínez-Romero C, Farias EF, Mayol X, Cano A and Hernández-Muñoz I. The polycomb group protein RING1B is overexpressed in ductal breast carcinoma and is required to sustain FAK steady state levels in breast cancer epithelial cells. Oncotarget 2014; 5: 2065-2076.
[41] Wang H, Niu X, Mao F, Liu X, Zhong B, Jiang H and Fu G. Hsa_circRNA_100146 acts as a sponge of miR-149-5p in promoting bladder cancer progression via regulating RNF2. Onco Targets Ther 2020; 13: 11007-11017.
[42] Yue F, Peng K, Zhang L and Zhang J. Circ_0004104 accelerates the progression of gastric cancer by regulating the miR-539-3p/RNF2 axis. Dig Dis Sci 2021; 66: 4290-4301.